THE EFFECTS OF MECHANICAL FORCING ON THE MEAN MERIDIONAL CIRCULATION AND TRANSFER PROPERTIES OF THE ATMOSPHERE

Wu Guoxiong (吴国雄)*

Institute of Atmospheric Physics, Academia Sinica, Beijing

and *Stefano Tibaldi*

European Centre for Medium-range Weather Forecasts, Reading, U.K.

Received May 31, 1986

ABSTRACT

Experiments using a quasi-geostrophic model and the ECMWF T21 spectral model with and without orography are performed to investigate the effects of mechanical forcing on the mean meridional circulation. Results show that mechanical forcing intensifies the horizontal poleward heat flux and redistributes the eddy angular momentum in the vertical, and that this changes significantly the intensity and location of the mean meridional circulation centres.

It is shown how the mean meridional circulation is set up in such a way to satisfy both the dynamical and thermodynamical transport requirements of the model atmosphere. Whenever external forcing changes the eddy fluxes, the Coriolis torques from the upper horizontal branches of the mean meridional circulations change to balance the extra divergence of eddy momentum flux, and additional adiabatic heating is produced by the vertical branches of the toroids to balance the extra divergence of eddy heat flux. The mean meridional circulation is, therefore, confirmed to be very sensitive to mechanical forcing, and can be used as an efficient tool to quantitatively diagnose the adequacy of the orographic representation of numerical forecasting and general circulation models.

I. INTRODUCTION

Charney and Eliassen (1949) pointed out that planetary waves can be excited by large-scale mountains. Later Charney and Drazin (1961) investigated atmospheric wave motions and found that only planetary scale waves can propagate upwards from the troposphere to the stratosphere, whereas synoptic-scale waves are trapped, or evanescent, in the vertical. For the vertically penetrating waves, the theory developed by Eliassen and Palm (1961) shows that, by extracting energy from the basic flow, they can amplify during their upward propagation. All these results suggest that the effect of mechanical (mountain) forcing on the atmosphere is not only to produce an additional torque at the surface, but also to change the vertical structure of atmospheric motions, especially by intensifying planetary waves in the upper troposphere and the lower stratosphere.

Since the 1960's, general circulation models (GCMs) have been used to investigate how

* This study was completed when the first author worked at the ECMWF as a visiting scientist.

mountains affect atmospheric motions. By comparing results from experiments with and without mountains, hereafter referred to as the MTN and NOM cases respectively, the influence of mountains could be evaluated. Using a model with 12 layers in the vertical, Kasahara, Sasamori and Washington (1973) found that orography does not significantly change the poleward eddy flux of momentum except in the upper stratosphere where the effect of the upper boundary condition is most critical. On the other hand, in mid-latitudes orography displaces the poleward transfer of sensible heat from the stratosphere to the upper troposphere. Also a substantial increase in wave energy flux due to the effects of mountains could be seen in the Northern Hemispheric stratosphere. With the inclusion of mountains the amplitude of wave-number 1 in the stratosphere increases two- or three-fold compared with the NOM case. Manabe and Terpstra (1974) used a 9-level model to conduct a similar experiment. They also found that, due to the increase in conversion from APE to KE in the MTN case, stationary waves are greatly amplified, as are the transfer properties of such stationary waves. All these model findings agree well with the available theoretical studies.

The main physical mechanism which, in the rotating frame of reference, can balance the generation of angular momentum at the ground surface and the eddy flux divergence/convergence of angular momentum taking place in the upper troposphere is the Coriolis torques acting on the north-south branches of the atmosphere by the mean meridional circulation. In other words, the mean meridional circulation is arranged in such a way that the Coriolis torque due to its lower branch balances the generation of angular momentum near the surface, and the one acting on its upper branch balances the divergence/convergence of eddy flux of angular momentum (*e.g.* Kidson *et al.*, 1969). Since mechanical effects (*e.g.* mountain forcing) can enhance the eddy heat flux and redistribute eddy momentum flux, and since the mean meridional circulation can only be maintained when the geostrophic and hydrostatic balances are continuously destroyed by diabatic heating and/or eddy transfer of heat and momentum (see also Eady, 1950; and Green, 1970), we can therefore expect orographic forcing to produce significant effects on the mean meridional circulation.

Section II contains a description of the results from a two-layer quasi-geostrophic model used to investigate some of the relevant physical mechanisms. In Section III, experiments using the ECMWF T21 global spectral model are described. Results from both these two models show that the enhanced angular momentum and heat flux in the MTN case have a large impact on the mean meridional circulations. Section IV summarises the main conclusions.

II. EXPERIMENTS WITH A QUASI-GEOSTROPHIC MODEL

In the framework of the quasi-geostrophic, Boussinesq model for the atmospheric long waves developed by White and Green (1982) and Wu (1984), the vorticity and thermodynamic equations become

$$\frac{D}{Dt}(\zeta+f)=f_*\frac{\partial w}{\partial z}-\nabla\cdot(\mathbf{V}'\zeta'), \tag{1}$$

$$\frac{D}{Dt}\left(\frac{\partial\psi}{\partial z}\right)+\frac{N^2}{f_*}w=-\gamma\left(\frac{\partial\psi}{\partial z}-\frac{\partial\tilde{\psi}}{\partial z}\right)-\nabla\cdot\left(\mathbf{V}'\frac{\partial\psi}{\partial z}\right)', \tag{2}$$

where $\frac{D}{Dt}$ is the total derivative in spherical geometry, ψ is the streamfunction, $\zeta=\nabla^2\psi$

is the geostrophic vorticity, f is the Coriolis parameter, primed quantities represent departures from a suitable low-pass time mean, $\tilde{\psi}$ indicates a reference state (e.g. a long-term time mean) and γ is a Newtonian-type heating/cooling coefficient. The last terms on the right hand side of both equations represent the transports by transient eddies (White and Green, 1982). For more details see White and Green (1982) and Wu (1984).

The model atmosphere is then divided into two equally deep layers, as shown in Fig. 1, and a rigid top at the tropopause ($z=H=10$ km) is assumed. Eqs. (1) and (2) applied at the middle layers and at the interface respectively, yield

$$\frac{D}{Dt_3}(\zeta_3+f)=\frac{-2f_0}{H}w_2-\nabla\cdot(\mathbf{V}_3'\zeta_3'),$$

$$\frac{D}{Dt_1}(\zeta_1+f)=\frac{2f_0}{H}(w_2-w_0)-\nabla\cdot(\mathbf{V}_1'\zeta_1'),$$

$$\frac{D}{Dt_2}\psi_s+\frac{HN^2}{2f_0}w_2=-\gamma(\psi_s-\tilde{\psi}_s)-\nabla\cdot(\mathbf{V}_2'\psi_s'),$$

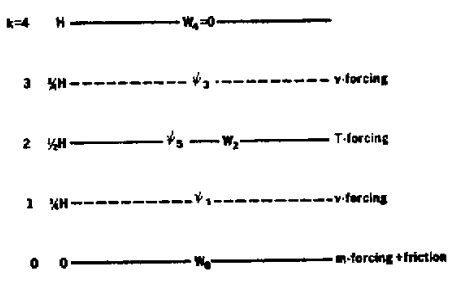

Fig. 1. Vertical resolution of the model atmosphere. Mechanical forcing is applied at the surface, thermal forcing at the middle level and vorticity forcing at levels 1 and 3.

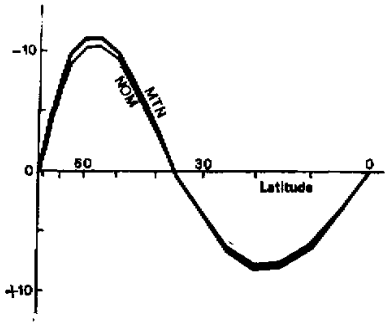

Fig. 2. Mean meridional mass circulation in the MTN and NOM cases for the quasi-geostrophic model. Units: 10^6 ton/s.

where $\psi_s=\psi_3-\psi_1$ represents the thickness between levels 3 and 1, and the substantial derivative is

$$\frac{D}{Dt_i}=\frac{\partial}{\partial t}+\mathbf{V}_i\cdot\nabla, \qquad i=1,2,3.$$

The vertical motion at the lower boundary w_0 is taken to be the sum of topographic lifting and Ekman pumping, therefore

$$w_0=\mathbf{V}_0\cdot\nabla h+\alpha\nabla^2\psi_0$$

where $\alpha=(\kappa/2f_0)^{\frac{1}{2}}$ and κ is the eddy viscosity coefficient, taken to be 10 m^2s^{-1} throughout the experiment. Quantities at the surface and top boundary are linearly extrapolated from their corresponding values at levels 1 and 3. The time increment is taken as six hours. All experiments are started from an atmosphere at rest and the integrations continue until a steady

state is reached. Results from this state, referred to as the model atmosphere, are then discussed. The diabatic heating field $-\gamma(T-\bar{T})$ contributes to about 1°C/d warming over the two ocean areas and cooling over the two land areas (continents). Mountains are represented in the model by ridges over the continents and valleys over the oceans. Further details about this model are described by Wu (1984).

We now want to examine the mean meridional circulation implied by this model. Using the zonally averaged continuity equation in spherical geometry (overbars indicate zonal mean quantities)

$$\frac{\partial \bar{w}}{\partial z}+\frac{1}{a\cos\phi}\frac{\partial}{\partial\phi}(\bar{v}\cos\phi)=0, \tag{3}$$

we define the zonal mean mass flux χ by

$$2\pi a^2\cos\phi\rho\bar{w}=\frac{\partial\chi}{\partial\phi}, \tag{4}$$

$$2\pi a\cos\phi\rho\bar{v}=-\frac{\partial\chi}{\partial z}. \tag{5}$$

The meridional distributions of χ in the MTN and NOM cases are shown in Fig. 2. Positive χ values correspond to the (direct) Hadley cell, whereas negative χ values represent the (indirect) Ferrel cell.

The intensity of the Ferrel cell in our simple model is about half of that found in the real atmosphere, as estimated for example by Palmen and Vuorela (1963). However, the Hadley cell, estimated as 230×10^6 ton/s in the real atmosphere, is reproduced far too weakly. This weakness is mainly due to the fact that our model is a geostrophic model in which f is used rather than (more properly)$\left(f-\frac{\partial u}{\partial y}\right)$, and$f$ has a constant value (f_0) typical of mid-latitudes. Hence the Coriolis effect in low latitudes is overestimated. Since the vertical westerly shear required to balance the zonal mean temperature difference is proportional to $f(v_3-v_1)$, then for a given temperature difference, a larger f must result in a smaller zonal mean meridional velocity. These features are also found in other models: using a two-level quasi-geostrophic model, Phillips (1954) investigated the general circulation on the β-plane and obtained a zonal mean meridional speed of 5 cm/s in the Hadley cell and about half of that in the Ferrel cell. Hollingsworth (1975) used spherical coordinates to investigate baroclinic instability and showed that, in the quasi-geostrophic model used by Phillips (1954), the mass flux in the Ferrel cell is about 50% larger than that in the Hadley cell. However, in a model designed by Lorenz (1960) which includes some non-geostrophic effects, the mass fluxes in the Hadley cell and in the Ferrel cell are very similar.

Another important reason for the weakness of the Hadley cell in our model is the absence of latent heat release since, to a large extent, the real atmosphere's Hadley cell is directly driven by latent heat released along the ITCZ. In their numerical simulation of the general circulation in the tropics, Manabe and Smagorinsky (1967) calculated the intensity of the direct cell for both dry and moist versions of the model, and compared them with the real atmosphere. In their moist run, the direct cell has an intensity of about 140×10^6 ton/s, but only 52×10^6 ton/s in the dry run. Despite these unrealistically large value, their experiment shows that condensation processes contribute significantly to the intensification of the tropical cell.

Referring back to Fig. 2, we see that both the Hadley cell and the Ferrel cell are intensified by the mechanical forcing. In order to explain this, we follow Holton (1979) and consider the diagnostic equations for the mean meridional circulation in our model. Upon setting

$$\bar{v} = -\frac{\partial \chi}{\partial z} \text{ and } \bar{w} = \frac{\partial \chi}{\partial y},$$

(note that for simplicity we have reverted back to plane geometry) and using the zonal mean continuity equation

$$\frac{\partial \bar{w}}{\partial z} + \frac{\partial \bar{v}}{\partial y} = 0,$$

the vorticity Eq. (1) and the thermodynamic Eq. (2) can be rewritten as

$$\frac{\partial}{\partial t}\left(\frac{\partial \bar{\psi}}{\partial y}\right) = \frac{\partial}{\partial y}(\overline{u^* v^*} + \overline{u' v'}) + f_0 \frac{\partial \chi}{\partial z}, \tag{6}$$

$$\frac{\partial}{\partial t}\left(\frac{\partial \bar{\psi}}{\partial z}\right) = -\frac{\partial}{\partial y}\left(\overline{v^* \frac{\partial \psi^*}{\partial z}} + \overline{v' \frac{\partial \psi'}{\partial z}}\right) - \frac{N^2}{f_0}\frac{\partial \chi}{\partial y} + \bar{Q}, \tag{7}$$

where $\bar{Q}$ is the zonal mean diabatic heating and starred quantities represent departures from zonal mean values (overbars). After eliminating the local variation terms in these two equations, we obtain a diagnostic equation for χ:

$$\nabla^2 \chi = \left(\frac{\partial^2 \chi}{\partial y^2} + \frac{f_0}{N^2}\frac{\partial^2 \chi}{\partial z^2}\right) \tag{8}$$

$$= -\frac{f_0}{N^2}\left[\frac{\partial^2}{\partial y^2}\left(\overline{v^* \frac{\partial \psi^*}{\partial z}} + \overline{v' \frac{\partial \psi'}{\partial z}}\right) + \frac{\partial}{\partial z}\frac{\partial}{\partial y}(\overline{u^* v^*} + \overline{u' v'}) - \frac{\partial \bar{Q}}{\partial y}\right].$$

This equation states that a meridional circulation is produced only when the geostrophic and hydrostatic balance are continuously destroyed either by diabatic heating or by the transfer properties of eddies. In other words, the ageostrophic mean meridional circulation is generated to balance the zonal mean diabatic heating; the transfer of angular momentum and heat by the transient eddies and/or stationary eddies restores the geostrophic and hydrostatic balances. For example, a net diabatic heating in the tropics and cooling in the polar region result in $\frac{\partial \bar{Q}}{\partial y} < 0$, so that $\chi > 0$; a direct Hadley cell is then produced. This diabatic heating requires an increase in thermal wind. In the absence of angular momentum transfer by eddies, Eq (6) shows that this increase in thermal wind can only be provided by the coriolis torque due to a direct cell. On the other hand, the adiabatic heating resulting from this direct cell acts against the diabatic effect so that the meridional temperature gradient is decreased. This process continues until a new geostrophic and hydrostatic balance is attained. Since the eddy heat transfer in mid-latitudes tends to decrease the meridional temperature gradient, a similar argument shows that an indirect cell in middle latitudes is again required in order to maintain geostrophic and hydrostatic balance.

The diabatic heatings in the MTN model and in the NOM model are almost identical, so they are of no relevance to the change of $\nabla^2 \chi$. The intensification of eddy heat transfer due to MTN forcing could be responsible for the increase of $\nabla^2 \chi$. However, in our present

experiments, this intensification has been minimised and therefore cannot account for the change of $\nabla^2\chi$.

The second term inside the square brackets of (8) represents the effect on the mean meridional circulation of the eddy transfer of angular momentum. In middle latitudes, the convergence of angular momentum increases with height. This, according to (8), will result in an indirect Ferrel cell.

Table 1 shows the maximum poleward eddy transfer of angular momentum in the upper and lower troposphere in the NOM and MTN cases. The vertical integral of the total eddy transfer of angular momentum (the last column) in these two cases is similar. However, due to the mechanical forcing, the transfer of angular momentum by transient eddies and stationary waves in the upper layer in the MTN case is increased, whereas that in the lower layer is decreased.

Table 1. The Maximum Poleward Transfer of Angular Momentum by Eddies(T_e)in the Upper (labeled 3) and Lower (labeled 1) Model Troposphere Layers in the NOM and MTN Cases (Units of Hadley)

	T_{e3}	T_{e1}	$T_{e3}-T_{e1}$	$T_{e3}+T_{e1}$
NOM	20.76	2.88	17.9	24
MTN	21.88	1.45	20.4	23

These changes in angular momentum transfer cause an increase in magnitude of the second term on the right hand side of (8), resulting in the intensification of both the Hadley and the Ferrel cells. Physically this can be interpreted in terms of the mountains strengthening the EP-flux and causing perturbations to develop more intensely in the upper troposphere. The intensified transfer by such perturbations then produces a stronger thermal wind (see Eq. 6), which requires a stronger meridional temperature gradient. Eq. (7) shows that in the absence of diabatic heating and eddy heat transfer, this can only be produced by adiabatic heating due to an extra indirect cell (vertical motion). On the other hand, the Coriolis torque exerted by this cell on the zonal flow tends to oppose the increase of thermal wind (see Eq. 6). Thereby new geostrophic and hydrostatic balances are reestablished through the intensified circulation. In other words, it is by this adaptation process that the Hadley and Ferrel cells are intensified by the mechanical forcing due to mountains.

Numerical experiments by Kasahara, Sasamori and Washington (1973) showed that the inclusion of mountain forcing in a GCM causes a substantial increase of eddy heat flux in the troposphere (see their Fig. 10). The change of the first term on the right-hand side of (8) due to the mechanical forcing must, therefore, contribute greatly to an increase of the intensity of $\nabla^2\chi$. On the other hand, there is no corresponding increase of eddy flux of angular momentum in the troposphere. We note that the decrease of angular momentum eddy flux in the MTN case in their experiments is strongest in the lower troposphere (see their Fig. 9). Therefore, the change of the second term on the right-hand side of (8) due to mechanical forcing must also correspond to an increase of $\nabla^2\chi$. Despite the uncertainty of the relative importance of these two terms, it is evident that the presence of mountains helps strengthening the mean meridional circulation.

III. EXPERIMENTS WITH THE ECMWF T21 SPECTRAL MODEL

To try to verify these ideas in the context of a general circulation model, we used the low-resolution (triangular truncation 21, 16 levels) version of the ECMWF spectral model (Simmons and Jarraud, 1984) to carry out a Manabe and Terpstra-type experiment. Two twin integrations were carried out to 60 days and the last 30 days were used to assess the results. One integration used a mean-type orography (MTN) and the other one had zero orography everywhere (NOM). The initial conditions were taken from 12 GMT, 1 January, 1983. The method of diagnosing the mean meridional circulation is the one described in Wu and Brankovic (1985).

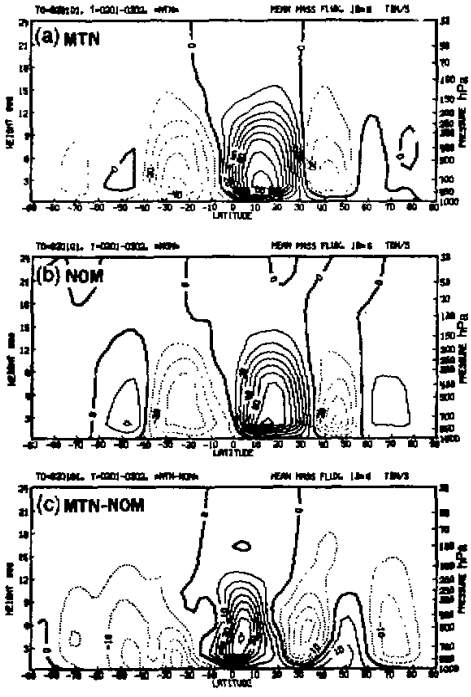

Fig. 3. Mean meridional mass circulation for the ECMWF T21 model. Positive centres correspond to direct cells in the Northern Hemisphere, but indirect cells in the Southern Hemisphere. Streamline interval: 10×10^{9} ton/s in (a) and (b), 5×10^{9} ton/s in (c). (a) MTN case; (b) NOM case and (c) difference between (a) and (b).

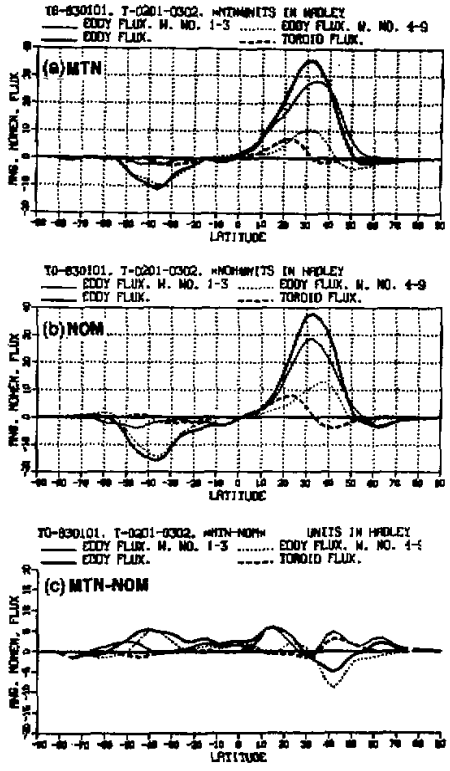

Fig. 4. Vertical integrals of angular momentum flux by wavenumbers 1—3 (light solid), 4—9 (dotted), all waves(thick solid) and the mean toroids (dashed). Units: Hadley (1 Hadley $=10^{18}$ kg m^2 s^{-2}).
(a) MTN case; (b) NOM case and (c) difference between (a) and (b).

The total time of integration is considerably larger than the kinetic energy consumption time typical of atmospheric conditions. This shou'd ensure that the details of the initial distribution of kinetic energy is not important and, therefore, the results should depend little on the initial conditions. On the other hand, the results are likely to depend critically on external forcings such as sea surface temperature distribution and mechanical forcing. The external diabatic forcing is representative of winter (January climatological SSTs and solar zenith angle), and so we can regard the integrations as being typical winter GCM experiments.

1. *The Mean Meridional Mass Flux*

Fig. 3 shows the mean meridional mass flux in the two different experiments and the difference field in between. In both cases, there are three cells in each Hemisphere. In the NOM case, the two tropical cells are separated near the equator, whereas in the MTN case the

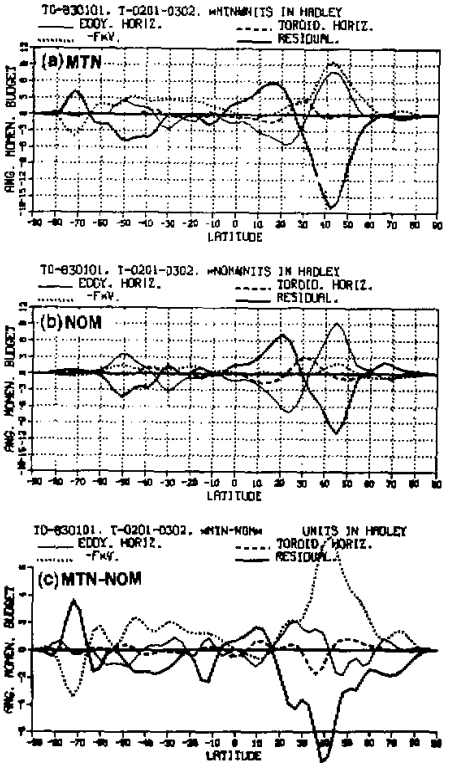

Fig. 5. Vertical integrals by the convergence of angular momentum flux by eddies (light solid) and toroids (dashed), and the residual interpreted as the angular momentum sources (thick)—for details see text.Units: Hadley.
(a) MTN case; (b) NOM case and (c) difference between (a) and (b).

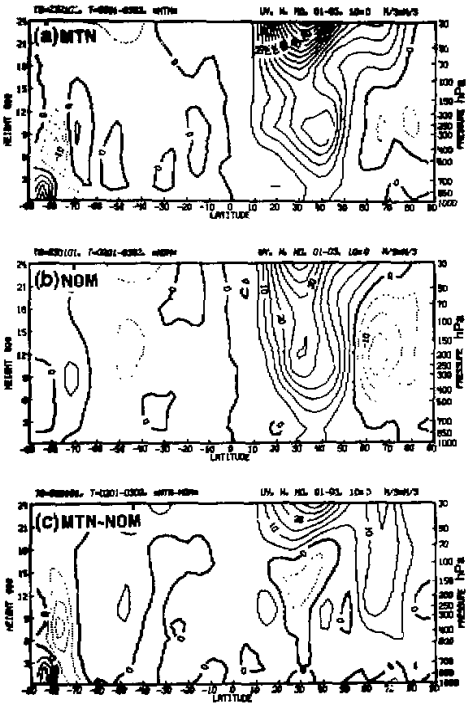

Fig. 6. Meridional cross-sections of momentum flux of $\overline{u^*v^*}$ by wavenumbers 1—3.Isopleth interval: 5 m^2s^{-2}.
(a) MTN case; (b) NOM case and (c) difference between (a) and (b).

Northern Hemispheric Hadley cell (and, consequently, the model's ITCZ) is shifted southwards by about six degrees; that is closer to its observed climatic position which is located at about 10°S (Kidson et al., 1969). As is well known, the extension of the Hadley cell from the winter hemisphere into the summer hemisphere has significant effects on the hemispheric balance of heat and moisture, and this seems, to a large extent, to be the result of mechanical forcing.

The intensities of the southern and northern Hadley cells are 41×10^6 and 87×10^6 ton/s respectively in the NOM case, whereas their counterparts in the MTN case are 57×10^6 and 99×10^6 ton/s. Compared with that of the northern Hadley cell of 140×10^6 ton/s obtained in the numerical experiments of Manabe and Smagorinsky (1967), and the estimates of 170×10^6 ton/s obtained by Kidson et al. (1969), and of 80×10^6 ton/s by Mintz and Lang (1955), our value in the MTN case does not deviate radically from previous calculations despite the fact that different models and diagnostic methods are employed. The relative increase of the Hadley cell due to the mechanical forcing is 14% in the Northern Hemisphere and 40% in the Southern Hemisphere. Fig. 3(c) shows changes both in position and in intensity. It is worthy of mention that the changes in the Southern Hemisphere are relatively small in comparison with those occurring in the Northern Hemisphere. This is in accordance with the fact that less mechanical forcing is exerted in the Southern Hemisphere. On the other hand, in the Northern Hemisphere the increase of the tropical direct cell reaches 43×10^6 ton/s, whereas that of the mid-latitude indirect cell reaches 24×10^6 ton/s. However, the latter is mainly due to the southward shift of the mean meridional circulation in the MTN case. These dramatic changes in the mass flux agree very well with the quasi-geostrophic theory discussed earlier.

It is also interesting to notice that there are four cells in the difference field in the Northern Hemisphere. In other words, the horizontal scale of the difference field is somewhat smaller than those of the mass flux field itself. As we will discuss later, this is due to the fact that the contributions to the mean meridional flux coming from eddies of different scales are latitude-dependent.

2. *The Angular Momentum Budget*

Fig. 4 shows the total vertical integral of angular momentum flux:

$$2\pi a^2\int_{30}^{1000}\overline{(u^*v^*}\cos^2\phi)\frac{dp}{g}\ .$$

The general picture in the two cases is not very different. They both show that planetary waves play a more important role than the shorter waves in transporting poleward angular momentum in the Northern Hemisphere, whereas wavenumbers 4—9 dominate the process in the Southern Hemisphere. In addition, the maxima of the total eddy flux do not change dramatically in the two cases. The difference flux (Fig. 4(c)) shows that, although the mechanical forcing decreases the poleward flux by wavenumbers 4—9 in both hemispheres, it increases the flux of planetary waves in the Northern Hemisphere and decreases it in the Southern Hemisphere. The total poleward eddy flux then increases over the northern tropics and high latitudes but decreases elsewhere. The only significant change in the toroidal flux occurs in the northern Ferrel cell, where in the MTN case the upper branch of the cell transfers less momentum southwards.

The expression for the vertical integral of the convergence of angular momentum flux is given below:

$$2\pi a^2\int_{30}^{1000}\frac{\partial}{\partial\phi}\cdot\overline{(u^*v^*}\cos^2\phi)\frac{dp}{g}\ .$$

Fig. 5 shows the contributions to this quantity from eddies and from meridional circulation separately, and their residual which indicates the likely distribution of the sources/sinks of angular momentum necessary to close the balance.

We see that angular momentum is generated in the tropics and dissipated in the mid-latitudes, and the generation or dissipation are, to a large extent, balanced by the divergence or convergence of angular momentum by eddies. From the difference between the two integrations (Fig. 5(c)) we find that, while mountains increase the eddy divergence of angular momentum in the equatorial belt and in high mid-latitudes, they increase the convergence in the latitude belt between 20° and 40° in both hemispheres. The substantial decrease of generation of momentum (torque) in the northern subtropics corresponds to the substantial decrease of surface easterlies taking place there as a result of the southward shift of the northern Hadley cell.

Figs. 6 and 7 show the meridional cross-sections of angular momentum flux $(\overline{u^*v^*})$ due to wavenumbers 1—3 and 4—9 respectively. Again we see that these results have some common features. For example, in both cases planetary waves are important in the Northern

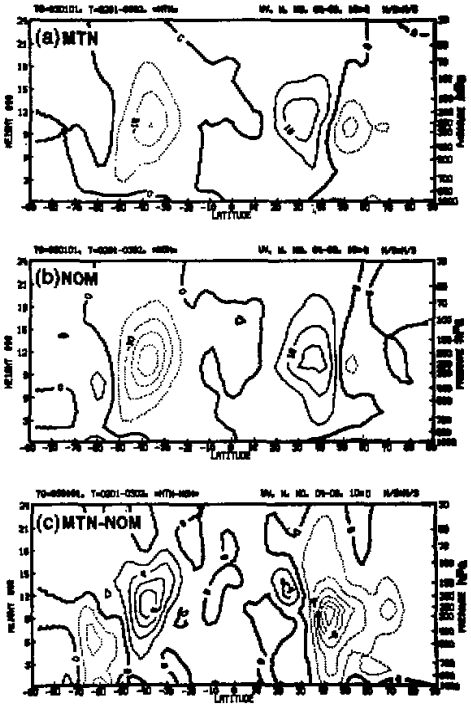

Fig. 7. Meridional cross-sections of momentum flux of $\overline{u^*v^*}$ by wavenumbers 4—9. Isopleth interval: 5 m^2s^{-2} in (a) and (b), 2 m^2s^{-2} in (c).
(a) MTN case; (b) NOM case and (c) difference between (a) and (b).

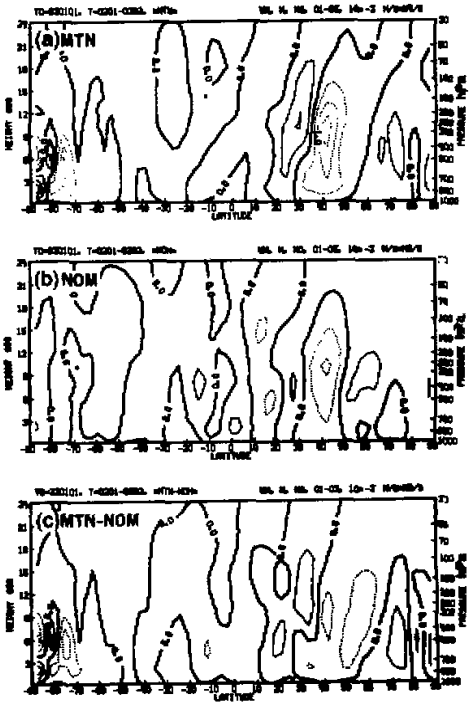

Fig. 8. Meridional cross-sections of vertical momentum flux of $\overline{u^*w^*}$ by wavenumbers 1—3. Isopleth interval: 5×10^{-4} hPa m s^{-2}.
(a) MTN case; (b) NOM case and (c) difference between (a) and (b).

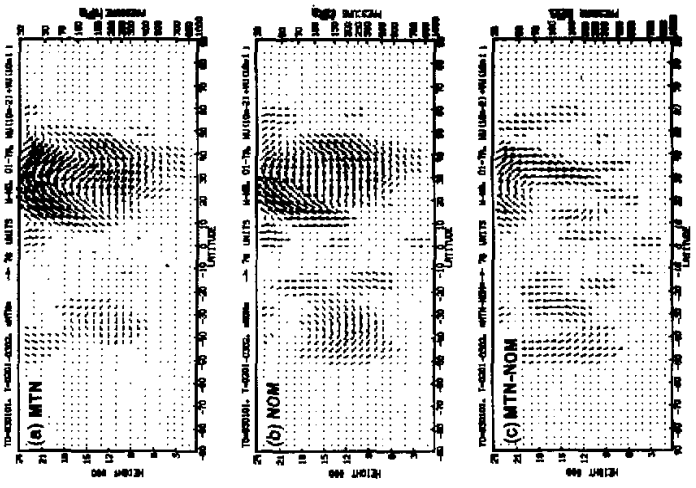

Fig. 10. Vector flux of momentum $(\overline{u^*v^*}\mathbf{i}+\overline{u^*w^*}\mathbf{k})\cos^2\phi$ by all waves. *Horizontal quantities have been scaled* down by a factor of 10, whereas vertical fluxes are amplified by a factor of 1000. (a) MTN case; (b) NOM case and (c) difference between (a) and (b).

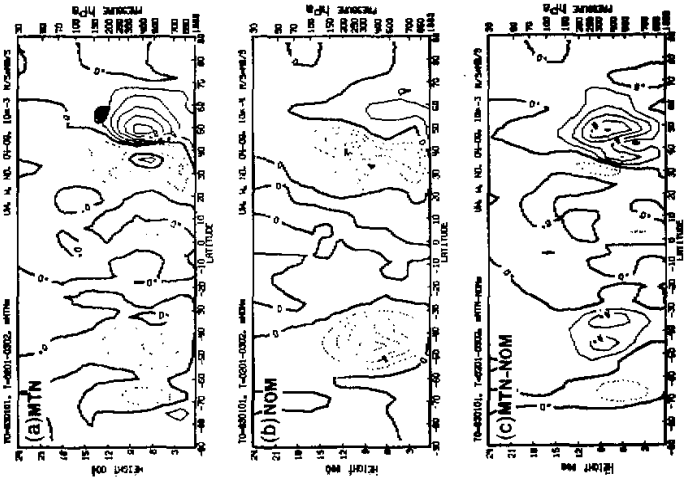

Fig. 9. Meridional cross-sections of vertical momentum flux of $\overline{u^*w^*}$ by wave-numbers 4—9. *Isopleth interval:* 2×10^{-4} hPa m s^{-2}. (a) MTN case; (b) NOM case and (c) difference between (a) and (b).

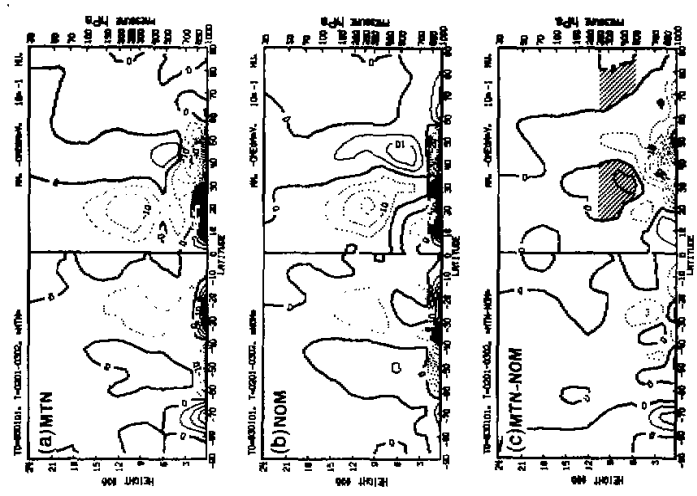

Fig. 12. Distribution of the negative angular momentum torque exerted upon the atmosphere from the meridional mass flux. Dotted and hatched areas denote the verification areas in the Northern Hemisphere corresponding to Fig. 3(c). Units: 0.1 Hadley.
(a) MTN case; (b) NOM case and (c) difference between (a) and (b).

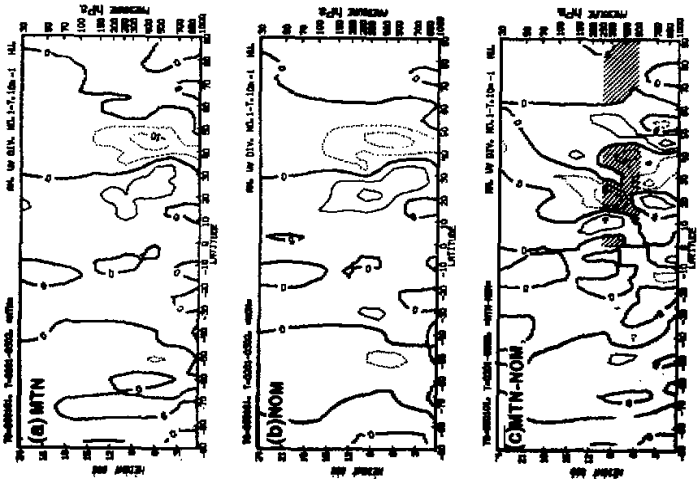

Fig. 11. Meridional divergence of horizontal flux of angular momentum by eddies. Dotted and hatched areas denote the verification areas in the Northern Hemisphere corresponding to Fig. 3(c). Units: 0.1 Hadley. (a) MTN case; (b) NOM case and (c) difference between (a) and (b).

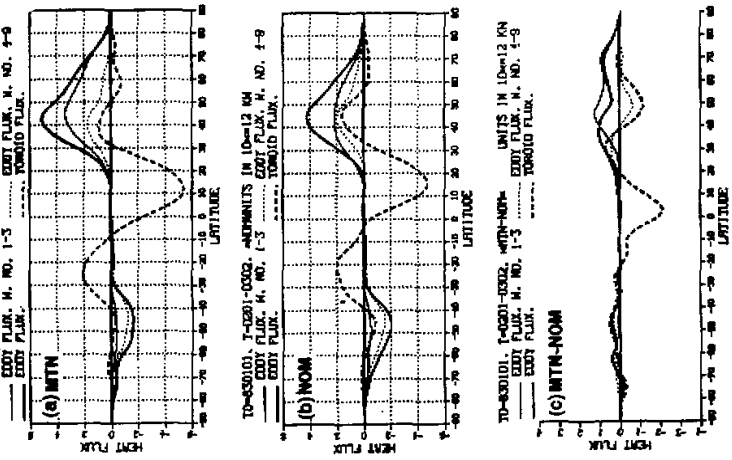

Fig. 14. Vertical integrals of sensible heat flux by waveunumbers 1—3 (light solid), 4—9 (dotted) and all waves (thick). Units: 10^{13} kw.
(a) MTN case; (b) NOM case and (c) difference between (a) and (b).

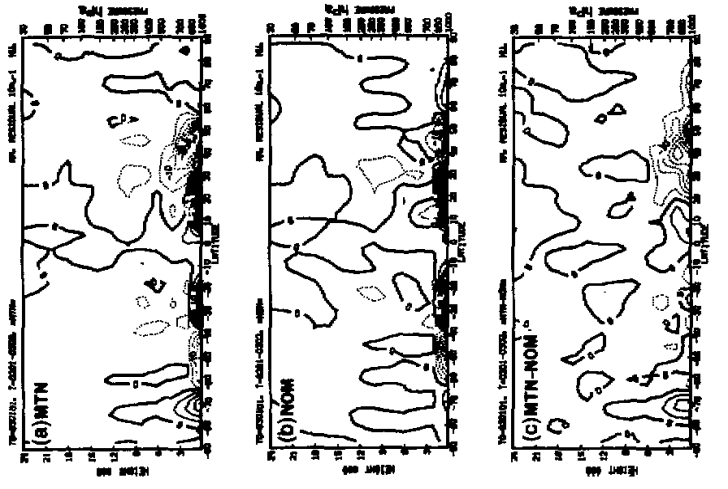

Fig. 13. Distribution of the residual interpreted as the angular momentum sources. Units: 0.1 Hadley.
(a) MTN case; (b) NOM case and (c) difference between (a) and (b).

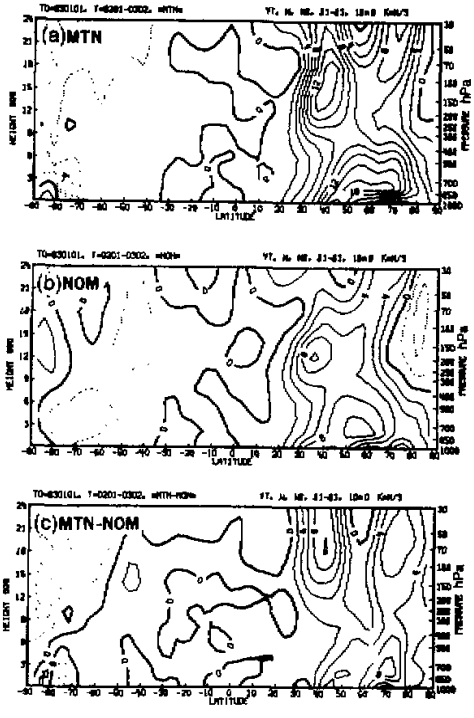

Fig. 15. Meridional cross-section of the horizontal sensible heat flux $\overline{v^*T^*}$ by wavenumbers 1—3. Isopleth interval: 2 K m s^{-1}.
(a) MTN case; (b) NOM case and (c) difference between (a) and (b).

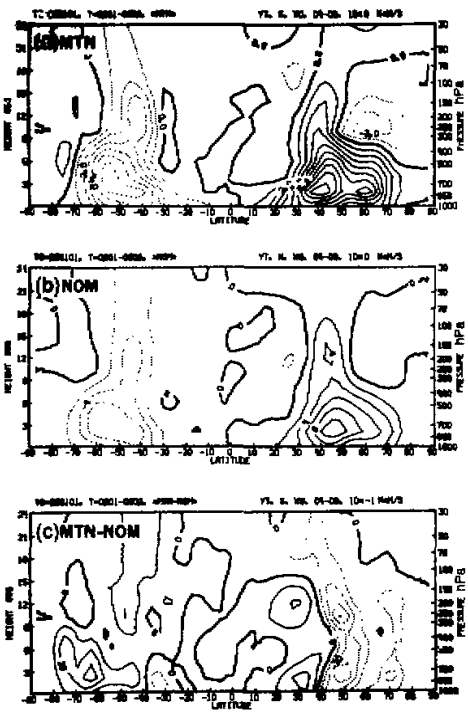

Fig. 16. Meridional cross-section of the horizontal sensible heat flux $\overline{v^*T^*}$ by wavenumbers 4—9. Isopleth interval: 1 K m s^{-1} in (a) and (c), 2 K m s^{-1} in (b).
(a) MTN case; (b) NOM case and (c) difference between (a) and (b).

Hemisphere, and shorter waves dominate the process in the Southern Hemisphere; yet the contributions from planetary waves can penetrate from the troposphere into the stratosphere, whereas the shorter waves are mainly trapped. The difference field for wavenumbers 1—3 (Fig. 6c) shows that the effects of mechanical forcing on such transfers are stronger in the upper troposphere and stratosphere in the mid-latitudes (especially in the Northern Hemisphere) and in high latitudes above 500 hPa. In the stratosphere, the two maxima of 34 m^2/s^2 and 16 m^2/s^2 are located at 36°N and 66°N respectively. The narrow negative belt around the tropopause level at about 30°N is indicative of a smaller horizontal north-south tilting of the waves there. In contrast to what takes place in the Northern Hemisphere, the mechanical forcing has a much smaller effect in the Southern Hemisphere, except near Antartica where a centre of -19 m^2/s^2 at about 400 hPa is observed. However, this has little effect on the overall angular momentum balance due to the effect of spherical geometry. The influence of orography on wavenumbers 4—9 (Fig. 7(c)) is very much confined to the upper troposphere and to mid-latitudes. The only positive centre in the Northern Hemisphere is

observed in the tropics. On the other hand, there is a substantial decrease of the poleward flux of momentum in the mid-latitudes. This is in accordance with the previous numerical results of Kasahara, Sasamori and Washington (1973).

The vertical momentum flux ($\overline{u^*w^*}$) due to the two wavenumber bands in the MTN and NOM integrations are shown in Figs. 8 and 9. The maxima due to the shorter waves are close to the middle troposphere, but those due to planetary waves are much higher, reaching up to the tropopause, especially in the MTN case. Consequently a large amount of momentum is transferred from the troposphere into the stratosphere by large-scale eddies. We notice that the effect of mountain mechanical forcing on the vertical transfer of angular momentum due to shorter waves is relatively small in the Southern Hemisphere; in contrast, it strongly intensifies the upward angular momentum flux due to planetary waves in the Northern Hemisphere mid-latitudes (Fig. 8(c)). This is quite consistent with the theory of Charney and Drazin (1961).

The two components of eddy flux of momentum in the vertical and in the horizontal are combined together to form a flux vector $[(\overline{u^*v^*}\mathbf{j}+\overline{u^*w^*}\mathbf{k})\cos^2\phi]$; some of the results are presented in Fig. 10. The effects of mechanical forcing on the flux due to planetary waves are hardly noticeable below 500 hPa (figures not shown). In the difference fields measurable values of the fluxes which cross the tropopause are found between 12°—30°S, 15°—35°N, and 50°—60°N, in good agreement with the latitudinal locations of the main parts of the Andes, Qomolangma, and of the Rockies respectively. The downward difference flux between 12°—35°N is also apparent in Fig. 8(c). For the eddy flux due to synoptic-scale waves the effects of mechanical forcing are mainly to be found in the troposphere. It is worthy of notice that, compared to those in the NOM case, the areas where the eddy fluxes occur in the MTN case are shifted equatorwards. The changes in the total eddy flux field (Fig. 10) are due to a large extent to planetary scale waves, except in the Southern Hemisphere troposphere, where the shorter waves play a more important role. From these cross-sections we find that the divergence of eddy momentum flux in the tropics and the convergence in the subtropics, and more prominently so in the Northern Hemisphere, are remarkably intensified by the orography. This, as we will discuss below, results in a significant intensification of the Northern Hemisphere mean meridional circulation.

The terms that dominate the angular momentum budget of the atmosphere are the convergence of eddy flux, the toroidal Coriolis torque, and the generation term. The first two terms are given by the following expressions

$$2\pi a^2 \frac{\partial}{\partial \phi}\overline{(u^*v^*}\cos^2\phi)\frac{\Delta\phi}{g},$$

$$-4\pi a^3 \Omega \bar{v}\sin\phi\cos^2\phi\Delta\phi\frac{\Delta p}{g},$$

whilst the generation is given by the residual in the angular momentum balance equation. These terms are shown in Figs. 11—13. The main sources, again, are shown to be concentrated near the surface. The weak residuals in the free atmosphere are due to the diffusion scheme used in the ECMWF model (Tiedtke, 1983), which has the property of removing angular momentum from the westerlies and converging it into the easterlies. Due to the horizontal geometry and the vertical density stratification the weak angular momentum sinks in the free atmosphere are usually observed in the equatorward and downward branches of the tropical jets. The main features depicted in Figs. 11—13 are similar to those discussed above, i.e.,

the generation near the surface and the divergence by eddies in the free atmosphere are closely balanced by the opposite effect of the Coriolis torques. Comparing Fig. 11(c) with Fig. 12(c), we find that it is also true that in the free atmosphere the additional convergence of eddy flux due to the insertion of orography is roughly balanced by the Coriolis torque of the difference toroids. In the Northern Hemisphere, for example, the two divergence areas in the eddy flux, i.e., south of 12°N and between 40°N and 60°N, coincide with the areas where there is a negative difference inertial torque; and the other two main eddy flux convergence areas are accompanied by the positive areas of Coriolis torque. These are in very good agreement with the locations of the difference cells displayed in Fig. 3(c).

We can therefore conclude that the changes in the mean meridional mass flux in these two experiments are to a great extent due to the changes of eddy angular momentum flux resulting from mechanical forcing. For example, the evidently enhanced eddy momentum flux from the tropics to higher latitudes in the MTN case requires a larger inertial Coriolis torque there, and this can only be accomplished by a more vigorous Hadley cell. In other words, the extra divergence of eddy momentum flux in the tropics requires a decrease in the thermal wind, in the absence of extra diabatic heating and eddy heat flux, this can only be achieved by adiabatic heatings caused by an intensification of the direct Hadley cell. At the same time, the additional inertial torque exerted by the additional direct circulations cancels some part of the extra eddy momentum divergence flux and a new thermal balance is then restored.

3. *Heat Budget*

Fig. 14 indicates the vertical integral of heat flux

$$2\pi a\int_{30}^{1000} C_p\ \overline{v^*T^*}\cos\phi\,\frac{dp}{g}$$

of wavenumbers 1—3, 4—9 and all waves. While mechanical forcing in the Southern Hemisphere decreases the poleward heat flux, in the Northern Hemisphere it substantially increases the flux due to wavenumbers 1—3 everywhere, and to wavenumbers 4—9 at low latitudes, but decreases that due to wavenumbers 4—9 at high latitudes.

Figs. 15 and 16 display the cross-sections of heat flux due to wavenumbers 1—3 and 4—9 respectively. The changes in the eddy heat flux of the second wavenumber band caused by the introduction of orography are relatively weak and less concentrated. However, those due to planetary waves are more confined to high latitudes and high levels. The high latitude centres are possibly connected with mountains in those areas, such as Greenland and the Rockies.

Fig. 17 shows the horizontal divergence of sensible heat flux due to all eddies. In both hemispheres the eddies transfer a substantial amount of heat from low latitudes to mid-latitudes. We notice that the difference field, as a function of latitude, shows a dipolar structure. This is nothing but the consequence of the latitudinal shifts of the lines of maximum convergence caused by the introduction of mountains and is also attributable to the fact that the weakening of the flux due to wavenumbers 4—9 and the strengthening of that for wavenumbers 1—3 occur at different latitudes (see Figs. 15(c) and 16(c)). It is also interesting to notice that the divergence-convergence pattern characteristic of the difference field, according to the requirements of thermal wind balance, must produce two additional indirect cells between 25°N and 45°N, and between 55°N and 75°N; and an extra direct cell between 45°N and 55°N. These are indeed those we have observed in the difference mass flux as shown in Fig. 3(c).

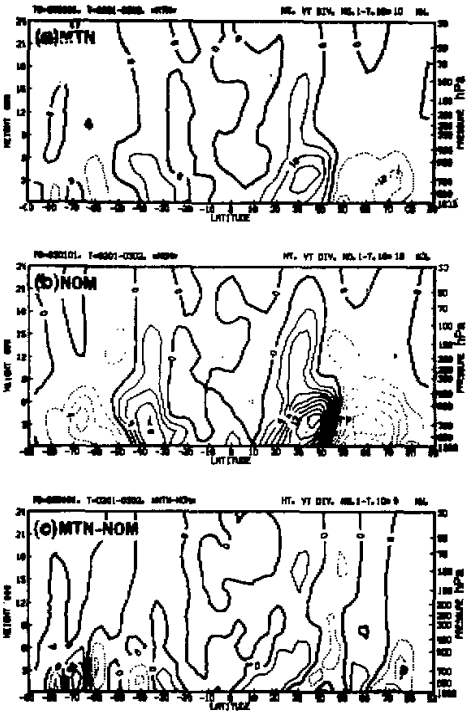

Fig. 17. Meridional divergence of the horizontal sensible heat flux of eddies. Units: 10^{10}kw in (a) and (b), 10^{9} kw in (c).
(a) MTN case: (b) NOM case and (c) difference between (a) and (b).

A consistent picture has therefore emerged which shows how the eddy heat flux and the eddy momentum flux cooperate in maintaining the mean meridional circulation. In other words, this circulation is organised in such a way that the inertial (Coriolis) torques exerted by the **horizontal branches** of the toroids balance the generation and transport of angular momentum. At the same time the adiabatic heating/cooling associated with the **vertical branches** is balanced by the generation and transport of heat in the free atmosphere.

IV. CONCLUDING REMARKS

(1) The mean meridional circulation of the atmosphere is a secondary type circulation which can only be maintained when the geostrophic and hydrostatic balances are continuously destroyed by eddy transfer of heat and/or momentum, or by diabatic heating. Since the sources of angular momentum in the free atmosphere are very weak, the mean meridional circulation is arranged in such a way that the inertial (Coriolis) torque exerted by its upper branch balances the divergence of eddy momentum flux. In addition, the intensity and position of the mean meridional cells must be organised in such a way that the adiabatic heating from their vertical branches are able to balance the combined effects of the diabatic heating taking place in the free atmosphere and of the divergence of the eddy heat flux.

(2) Since mechanical forcing enhances horizontal eddy heat fluxes and tends to

concentrate the eddy momentum flux to the upper layers of the atmosphere and to high latitudes, the intensity of the mean meridional circulation is altered significantly by it. In the framework of a quasi-geostrophic model, the introduction of mountains enhances the eddy poleward angular momentum transports at upper levels, while decreasing it at lower levels and thereby inducing, via the implied thermal wind adjustment, an intensification of both the Hadley and Ferrel cells.

(3) The introduction of mountains in a twin experiment using the ECMWF T21 spectral model shows a large impact: the model's ITCZ is shifted southward by approximately six degrees of latitude, the intensity of the Hadley cell is increased by approximately 15% in the Northern Hemisphere and 40% in the Southern Hemisphere, the Ferrel cells in both hemispheres are slightly weakened in intensity and the one in the Northern Hemisphere is displaced equatorward. There is good qualitative agreement between the results of the simple quasi-geostrophic model and the GCM results.

(4) Mountains are confirmed to be one important factor in the angular momentum budget in the atmosphere. The effect whereby mountains, by increasing the coupling between the solid earth and the atmosphere, and forcing extra meridional circulation to satisfy angular momentum balance requirements is confirmed as the dominating one.

(5) The effects of mechanical forcing in the Southern Hemisphere are much smaller (as should be expected) and confirm previous results.

(6) The mean meridional circulation and the angular momentum budget are shown to be very sensitive to mechanical forcing and can, therefore, be used as a powerful tool to diagnose the impact of orographic forcing and, consequently, the adequacy of the representation of mountains in GCMs.

We would like to thank Dr C. Brankovic for assistance in manipulating ECMWF archive data. We are also indebted to Dr U. Cubasch for assistance in running the two experiments. Our thanks are due to Dr J.S.A. Green for several discussions on the quasi-geostrophic experiments, and to Dr G. Shutts for stimulating discussions. Dr R. Riddaway carefully read the manuscript and improved it considerably.

The first author expressed his great thanks to the staff at ECMWF for their kindly offering all useful facilities and helps.

REFERENCES

Charney, J.G., and Drazin, P.G. (1961), Propagation of the planetary-scale disturbance from the lower into the upper atmosphere, *J. Geophys. Res.*, **66**: 83—109.

Charney, J.G., and Eliassen, A. (1949), A numerical method for predicting the perturbations of the middle latitude westerlies, *Tellus*, **1**: 20—54.

Eady, E.T. (1950), The cause of the general circulation of atmosphere, *Roy. Meteor. Soc. Cent. Proc.*, 156—172.

Eliassen, A., and Palm, E. (1961), On the transfer of energy in stationary mountain waves, *J. Geof. Publ.*, **22**: No. 3, 1—23.

Green, J.S.A. (1970), Transfer properties of the large-scale eddies and the general circulation of the atmosphere, *Quart. J. Roy. Meteor. Soc.*, **96**: 157—185.

Hollingsworth, A. (1975), Baroclinic instability of a simple flow on the sphere, *Quart. J. Roy. Meteor. Soc.*, **101**: 495—528.

Holton, J.R. (1979), An Introduction to Dynamic Meteorology, Academic Press.

Kasahara, A., Sasamori, T. and Washington, W.M. (1973), Simulation experiments with a 12-layer stratospheric global circulation model, I. Dynamical effect of the earth's orography and thermal influence of continentality, *J. Atmos. Sci.*, **30**: 1229—1251.

Kidson, J.W., Vincent, D.G. and Newell, R.E. (1969), Observational studies of the general circulation of the tropics: long term mean values, *Quart. J. Roy. Meteor. Soc.*, **95**: 258—287.

Lorenz, E.N. (1960), Energy and numerical weather prediction, *Tellus*, **12**: 184—193.

Manabe, S., and Smagorinsky, J. (1967), Simulated climatology of a general circulation model with a hydrologic cycle (II. Analysis of the tropical atmosphere), *Mon. Wea. Rev.*, **95**: 155—169.

Manabe, S., and Terpstra, T.B. (1974), The effects of mountains on the general circulation of the atmosphere as identified by numerical experiments, *J. Atmos. Sci.*, **31**: 3—42.

Mintz, Y., and Lang, J. (1955), A model of the mean meridional circulation, Final Report, AF 19(122)—48, General Circulation Project, Paper No. VI, University of California at Los Angeles.

Palmen, E., and Vuorela, L. (1963), On the mean meridional circulations in the Northern Hemisphere during the winter season, *Quart. J. Roy. Meteor. Soc.*, **89**: 131—120.

Phillips, N.A. (1954), Energy transformations and meridional circulations associated with simple baroclinic waves in a two-level quasi-geostrophic model. *Tellus*, **6**: 273—286.

Simmons, A.J. and Jarraud, M. (1983), The design and performance of the new ECMWF operational system, ECMWF Seminar on Numerical Methods for Weather Prediction, 5—9 September, 113—164.

Tiedtke, M. (1983), Winter and summer simulations with the ECMWF model, ECMWF Workshop on Intercomparison of Large-Scale Models Used for Extended Range Forecasts, 30 June –2 July 1982, 263—314.

White, A.A., and Green, J.S.A. (1982), A non-linear atmospheric long-wave model incorporating parmaterisations of transient baroclinic eddies, *Quart. J. Roy. Meteor. Soc.*, **108**: 55—85.

Wu, Guo-xiong (1984) The Non-linear response of the atmosphere to large-scale mechanical and thermal forcing. *J. Atmos. Sci.* **41**: 2456—2476.

Wu, Guo-xiong and Brankovic, C. (1985), General Circulation diagnostics package, ECMWF Tech. Memo. No. 96, 35pp.